Optimizing Heating Load Prediction For Enhanced Energy

Yijia Yuan, Kailun Chen, Yujie Wu, Jian Wang, Yue Sheng, Jiahui Li, and Baohua Shen*

Information Engineering College, Hangzhou Dianzi University, Hangzhou 311305, Zhejiang, China

* *Corresponding author. E-mail: shen_baohua@163.com*

Received: Feb. 13, 2024; Accepted: May 26, 2024

Energy conservation and emissions reduction are pivotal goals that hinge on precise energy consumption estimating and the assessment of retrofit options. Prioritizing energy-efficient practices in building management has gained significance in both theoretical research and practical applications. This ongoing research seeks to deliver a comprehensive solution by amalgamating advanced optimization algorithms with meticulous prediction of heating load (HL), addressing the pressing need for accuracy in this domain. The investigation delves into the intricate realm of HL systems, where the intricacies of energy optimization present diverse challenges necessitating thorough exploration and innovative problem-solving approaches. Two meta-heuristic techniques, the Adaptive Opposition Slime Mould Algorithm (AOSMA) and the Snake Optimizer (SO), have been combined to improve the accuracy of the K-Nearest Neighbour (KNN) model. These algorithms scrutinize HL data collected from various soil types via prior stability tests to validate the models. Three unique models are presented in the study: KNSO, KNAO, and an independent KNN model. All three models provide insightful information for accurate HL prediction. Notably, the KNAO model is a standout performance with an RMSE value of 0.8003 and an R^2 value of 0.993 which is remarkably low. These results underscore the effectiveness of the KNAO model in predicting HL outcomes with remarkable accuracy.

Keywords: Heating Load; K-Nearest Neighbor; Snake Optimizer; Adaptive Opposition Slime Mould Algorithm

http://dx.doi.org/10.6180/jase.202505_28(5).0001

1. Introduction

In today's society, the building sector occupies a prominent position as a significant energy consumer and producer of carbon dioxide emissions. Due to this industry's high energy requirements, experts are adamant about the need for energy conservation. Within buildings, heating consumes a sizable portion of this energy [1, 2]. For energy modeling, it is essential to predict a building's energy usage precisely, but this approach frequently underestimates the performance of actual buildings [3]. To estimate the amount of energy used in buildings, traditional energy models use engineering calculations and physical laws. These models are suitable for preliminary analysis [4]. However, these models frequently show a significant discrepancy between their predictions and actual energy consumption, occasionally even doubling or tripling the estimates. Numerical simulation methods are used to simulate building energy use to deal with this problem. These simulations are useful for providing insights, but they fall short of capturing the nuances of the real world [5, 6].

Artificial intelligence (AI) and machine learning (ML) are then applied in this situation. Simulators can assist in overcoming the difficulties involved in implementing ML and AI models for improving building energy efficiency by carefully analyzing the limitations of prior research [7]. The prediction of heating load (HL) and total building energy consumption may be transformed by ML and AI models [8, 9].

More accurate energy forecasts are made possible by these models' abilities to analyze sizable datasets, identify

patterns, and adjust to the complexities of the real world. To make sure that buildings are secure, energy-efficient, and comfortable, the heating, ventilation, and air conditioning (HVAC) industry is essential [10, 11]. Within this sector, the crucial subfield known as HL focuses on heating systems and the parts that make them up [12]. A wide range of heating technologies are included in HL, including conventional ones like furnaces and boilers, as well as cutting-edge ones like heat pumps, radiant heating, and solar heating. It is impossible to overstate how important HL is given that heating can consume up to 30% of a building's energy and is necessary for maintaining comfortable indoor environments, especially in colder climates [13, 14].

The healthcare industry has advanced significantly thanks to a growing focus on sustainability and energy efficiency. Due to this, high-efficiency heating systems, smart thermostat integration for precise temperature control, and improved insulation techniques to reduce heat loss have all been developed [15]. Additionally, eco-friendly alternatives like solar and geothermal heating have gained popularity as eco-friendly alternatives, minimizing the environmental impact of heating systems [16]. To ensure optimal performance and energy savings, experts in the HL sector are crucial in designing, installing, and maintaining these heating systems. The HL industry is still developing as the world struggles with the effects of climate change and the pressing need for energy conservation [17, 18]. It aims to offer effective and environmentally friendly heating solutions to the construction sector. Since they enable more precise predictions, improved energy management, and increased sustainability in the area of heating and building energy consumption, ML and AI are expected to play a transformative role in achieving these goals [19, 20].

Renowned innovators Kim and Cho [21] have pioneered a groundbreaking neural network aimed at revolutionizing the prediction of residential energy consumption. Their inventive model ingeniously combines Long Short-Term Memory (LSTM) and Convolutional Neural Network (CNN) architectures, effectively capturing spatial and temporal intricacies. This neural network emerges as a superior performer, surpassing conventional forecasting methods and offering unparalleled accuracy in predicting electric energy consumption for residential spaces. The proposed CNN-LSTM neural network, specifically tailored for housing energy consumption forecasting, stands as a testament to their visionary approach. In tandem, Moradzadeh et al. [22] contribute to the field by predicting heating and cooling loads with Support Vector Regression (SVR) and Multilayer Perceptron (MLP) models. Notably, the MLP method achieves an outstanding R-value of 0.9993 in predicting HL. This research introduces an advanced methodology that utilizes artificial neural networks and ML applications, specifically MLP and SVR techniques, to forecast heating and cooling loads and optimize energy consumption in residential buildings. These technological strides collectively affirm the transformative potential of advanced computational methods in elevating the precision and efficiency of residential building energy consumption predictions. In yet another important study, Roy et al. [23] introduced a deep neural network (DNN) model specifically designed to forecast the cooling and heating demands of residential buildings. In addition, minimax probability models, machine regression (MPMR), gaussian process regression (GPR), and gradient-boosted machine (GBM) were assessed in this research in relation to the DNN model. When it came to estimating cooling and heating loads, the DNN and GPR models clearly showed the most variation accounted for (VAF). Afzal et al. [24] addressed the difficult problem of predicting building energy consumption in a previous study, with a focus on heating and cooling applications. To carefully adjust and improve the hyperparameters related to the MLP model, their approach combined eight meta-heuristic algorithms with multilayer perceptron neural networks. The results of their exhaustive analysis were astounding: the MLPPSOGWO model, which stands for MLP-Particle Swarm Optimization-Grey Wolf Optimizer, had the greatest overall R^2 values (0.998) for the heating load. It continuously exhibits the highest level of precision, accuracy, and computing efficiency, making it the top performer.

In this scholarly investigation, an innovative ML and AI methodology is introduced. The primary objective of this approach is to attain the utmost precision and optimization in predictive outcomes. This is achieved through the meticulous customization of a hybridization method, strategically devised to amplify the efficacy of K-nearest neighbor (KNN)–based models, thereby ensuring the highest degree of reliability in prognostications. Pioneering hybrid models signify a noteworthy departure from conventional methodologies, establishing new benchmarks in predictive analytics. Thorough evaluations have been rigorously conducted to objectively evaluate their capabilities, encompassing both autonomous and hybrid configurations. This multifaceted approach has been instrumental in mitigating potential biases inherent in results, thereby affording a more nuanced perspective on the effectiveness of models.

Furthermore, a conscious decision was made to harness the unique strengths of two distinct optimization techniques, namely the Snake Optimizer (SNO) and the Adaptive Opposition Slime Mould Algorithm (AOSM), in the

Table 1. The statistical properties of the input variable of heating

Variables	Indicators				
	Category	Min	Max	Avg	St. Dev.
Relative Compactness	Input	0.62	0.98	0.764	0.106
Surface Area	Input	514.5	808.5	671.7	88.09
Wall Area	Input	245	416.5	318.5	43.63
Roof Area	Input	110.25	220.5	176.6	45.17
Overall Height	Input	3.5	7	5.25	1.751
Orientation	Input	2	5	3.5	1.119
Glazing Area	Input	0	0.4	0.234	0.133
Glazing Area Distribution	Input	0	5	2.813	1.551
Heating	Output	6.01	43.1	22.31	10.09

formulation of hybrid models. This strategic choice leverages the distinct attributes of each optimizer, thereby enhancing the overall performance of predictive systems. The research stands as a testament to the unrelenting pursuit of excellence in predictive analytics, auguring a promising trajectory in the domain of HL prediction.

2. Materials and methodology

2.1. Data gathering

Solid and trustworthy data is essential to ensuring the validity and effectiveness of the methods introduced in this study. This study used the data used to train the intelligent models from published research. This data offers the vital information required to put the suggested strategies into practice and assess how well they foresee the heating requirements of buildings. Here is a summary of the main ideas raised:

2.1.1. Data Partitioning

To ensure the validity and efficacy of the study's approaches, the data was divided into three subsets:

- *Training Set (70%)*: This subset, consisting of 70% of the data, is used to train the predictive model.
- *Validation Set (15%)*: This subset, consisting of 15% of the data, is used to fine-tune model parameters and prevent overfitting.
- *Testing Set (15%)*: This subset, also 15% of the data, is kept separate to evaluate the model's performance on unseen data.

2.1.2. Input Variables

A KNN model was used in the study to forecast Heating behavior. Eight important energy production input variables were taken into account for this:

- *Relative Compactness*: The surface area-to-volume ratio measures a building's compactness, with higher values indicating more efficient designs.
- *Surface Area*: The total exterior surface area is crucial for determining the heat exchange between the building and its surroundings.
- *Roof Area*: Roof area refers to the surface area of a building, influencing heat absorption and insulation, crucial for heating.
- *Wall Area*: The wall area, which signifies the surface area of a building, is significantly influenced by the material and insulation used in its walls.
- *Orientation*: Building orientation influences sunlight and solar heat gain, affecting heating requirements.
- *Overall Height*: The variable pertains to the height of a building, as taller structures may have varying heating requirements due to variations in air circulation and temperature distribution.
- *Glazing Area*: The glazing area, including windows, frame, and sash components, is influenced by the type and quality of glazing, which affects heat transfer, insulation, and natural lighting.
- *Glazing Area Distribution*: The arrangement of windows within a building significantly impacts its exposure to sunlight and outdoor conditions.

2.1.3. Dataset

This investigation utilizes a continuation of a previous research dataset for training intelligent models, which is crucial for implementing strategies and evaluating their ability to predict building heating needs.

2.1.4. Statistical Analysis

The study conducted a statistical analysis of the dataset, using metrics containing averages, standard deviation, minimum, and maximum values to understand its characteristics and distribution. Table 1 displays the statistical properties of both input and output variables, while Fig. 1 depicts a histogram illustrating their relationship.

The study utilizes an energy production dataset for training, validation, and testing a KNN model for predicting building heating behavior, utilizing statistical analysis for better understanding.

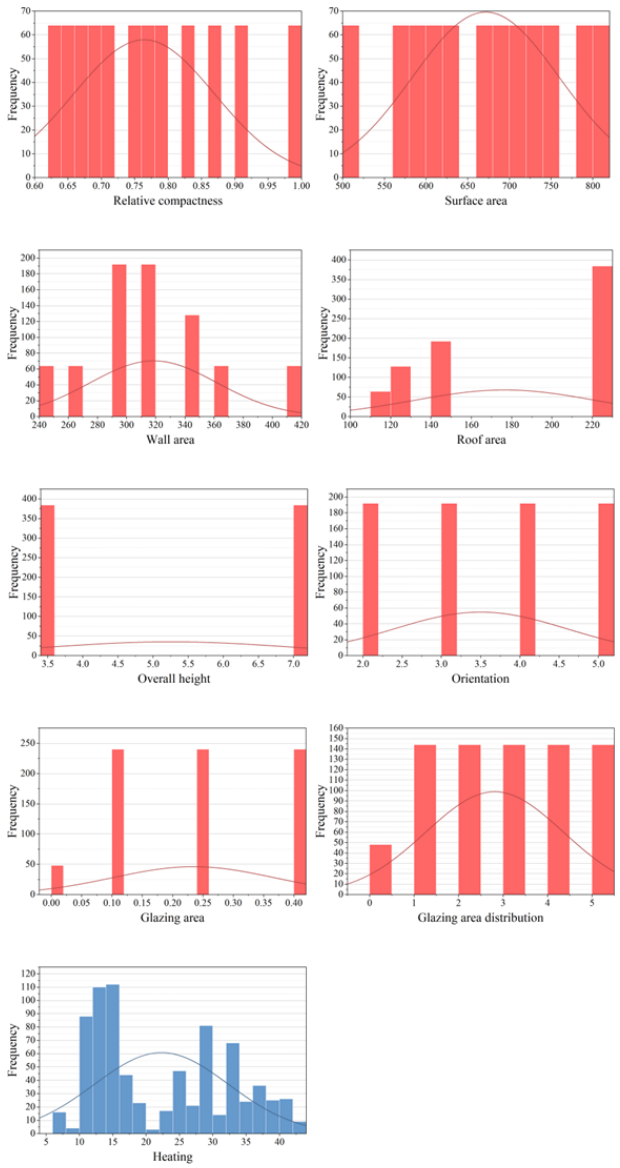

Fig. 1. The histogram illustrates the relationship between the input and output variables

2.2. K-nearest neighbor's (KNN)-based

According to the input that occurs the most frequently from K data points closest to the test point, the KNN algorithm estimates outcomes [25]. It is critical to handle the normalization of these parameters employing Eq. (1) prior to applying the process.

$$x_{\text{normalization}} = \frac{x - \text{Min}}{\text{Max} - \text{Min}} \tag{1}$$

Subsequently, the test and data points' Euclidean distance is calculated by Eq. (2).

$$Hx_i, x_j = \sum_{h=1}^{m} x_i^{(h)} - x_j^{(h)^2}{}^{\frac{1}{2}} \tag{2}$$

Utilizing the Euclidean distance and m as the number of argument points, Eq. (2) defines the distance H between the original data points (x_i) and the test point $\left(x_j\right)$. By Eq. (3), that is essential for modifying the Euclidean distance for all parameters to remove the inconsistent effects of indoor thermal parameters on thermal comfort, as different parameters have different influences on thermal comfort even when the same value is altered [26].

$$Hx_i, x_j = \sum_{h=1}^{m} w_h * x_i^{(h)} - x_j^{(h)^2}{}^{\frac{1}{2}} \tag{3}$$

The equation provides the weight (w_h) allocated to each indoor thermal parameter that
affects thermal comfort. To find the K data points that are closest to the test point, distances are computed. The input that appears the most often among these K data points is then considered to represent the feedback provided by the participants at the current test point. The K value, which determines the number of required dataset points, may be found by crossvalidation. Selecting a K value that is halfway between the two extremes is essential. If K is too small, the model could be very sensitive to sample points around the test point, which would result in an excessive quantity of noise point interference. However, the accuracy of the model may decrease if K is set too high [27]. In Fig. 2, the KNN flowchart is displayed.

2.3. Snake optimizer (SO)

The snakes' mating rituals serve as an inspiration for the SO algorithm. When it is cold outside, and there is food, animals mate. Otherwise, the snakes concentrate on finding food or eating what they already have. The search process is divided into two phases based on this information: exploitation and exploration. When environmental factors like food and cold places are absent, the snake searches for food in its surroundings during the exploration phase [28].

- Initialize

As with all metaheuristic algorithms, SNO initiates by creating a random population distributed uniformly to

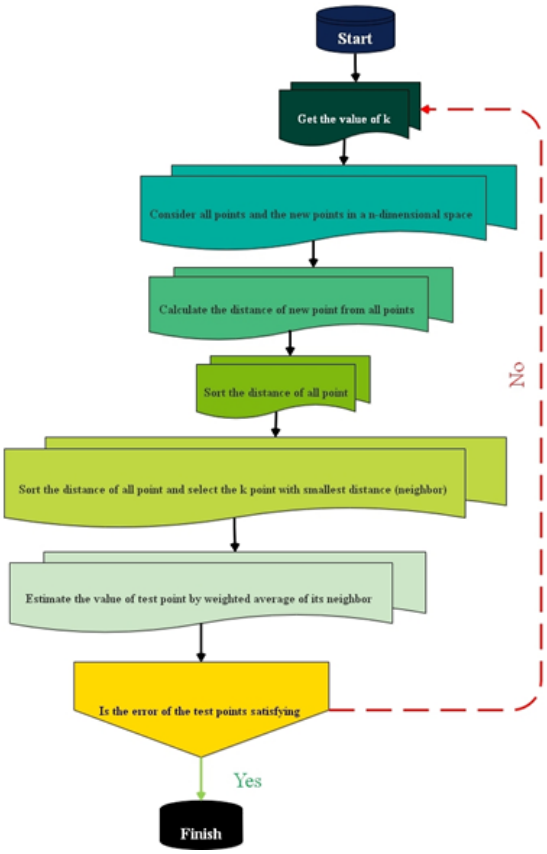

Fig. 2. The flowchart of the KNN model

kickstart the optimization process. The following Eq. (4) yields the initial population:

$$x_i = x_{\min} + \text{ rand } \times (x_{\max} - x_{\min}) \tag{4}$$

The position of the ith individual, x_i, can be determined using the equation, where rand is a random number between 0 and 1 , and $x_{\max}$ and $x_{\min}$ represent the upper and lower bounds of the problem, alternatively [28].

- Search Phase

When F is less than 0.25 , the snake explores by adjusting its position based on its current location and selecting a random point. To model food quality, temperature, and the search phase, the following calculations can be employed by Eqs. (5) to (7):

$$F = s_1 \times \exp\left(\frac{r-R}{R}\right) \tag{5}$$

$$\text{Temp } = \exp\left(\frac{-r}{R}\right) \tag{6}$$

$$X_i(t+1) = X_{\text{rand}}(t) \pm s_2 \times B \times ((X_{\max} - X_{\min}) \times \text{ rand } + X_{\min}) \tag{7}$$

In the context presented, the constants s_1 and s_2 are defined as 0.5 and 0.05, respectively. Here, r represents the current repetition, while R signifies the maximum number of repetitions. Additionally, X_{rand} denotes the randomly determined position, and rand signifies a randomly generated number ranging from 0 to 1 . The ability to locate food, denoted as B, is further elaborated as follows:

$$B = \exp\left(\frac{-q_{\text{rand}}}{q_i}\right) \tag{8}$$

In this context, q_{rand} represents the fitness of X_{rand} , while q_i denotes the fitness of the individual at the $i-$ th position.

- Exploitation phase

When both F is greater than 0.25 , and the temperature exceeds 0.6 , the snake's movement will be exclusively directed toward the food source. This movement can be quantified through the following calculation by Eq. (9):

$$X_{i,j}(t+1) = X_{\text{food}} \pm s_3 \times \text{ Temp } \times \text{ rand } \times \left(X_{\text{food}} - X_{i,j}(t)\right) \tag{9}$$

In this context, $X_{i,j}$ represents the position of the snake, X_{food} denotes the optimal position and s_3 corresponds to a constant value of 2 . When the temperature falls below 0.6 , the snake enters either the fight mode or the mating mode, which can be defined as per Eq. (10):

$$X_i(t+1) = X_i + s_3 \times A \times \text{rand} \times (F \times X_{\text{best}} - X_i(t)) \tag{10}$$

In this scenario, X_i refers to the position at the $i-th$ iteration, X_{best} signifies the most optimal position, and A represents the capability to engage in combat. The computation of A can be expressed as follows:

$$A = \exp\left(\frac{-q_{\text{best}}}{q_i}\right) \tag{11}$$

In this context, q_{best} represents the highest fitness value, while q_i denotes the fitness of the individual. The process of mating mode can be determined through the following calculation:

$$X_i(t+1) = X_i + s_3 \times G \times \text{rand} \times (F \times X_i(t)) \tag{12}$$

In this context, G represents the mating capability. This can be quantified using the following calculation:

$$G = \exp\left(\frac{-q_i}{q_i}\right) \tag{13}$$

Upon successful egg hatching, the protocol involves selecting the least proficient snake and replacing it:

$$X_{\text{worst}} = X_{\min} + \text{ rand } \times (X_{\max} - X_{\min}) \tag{14}$$

Here, the worst individual is indicated by X_{worst} .

The directional flag operator $\pm$, often referred to as the diversity factor, possesses the capacity to enhance or diminish the positional solution, thereby increasing the likelihood of the agent altering its direction and effectively exploring the given space from various perspectives. This parameter is of the utmost importance in meta-heuristic algorithms, which are inherently built to include randomness for enhanced diversification. The flowchart of the SO is displayed in Fig. 3.

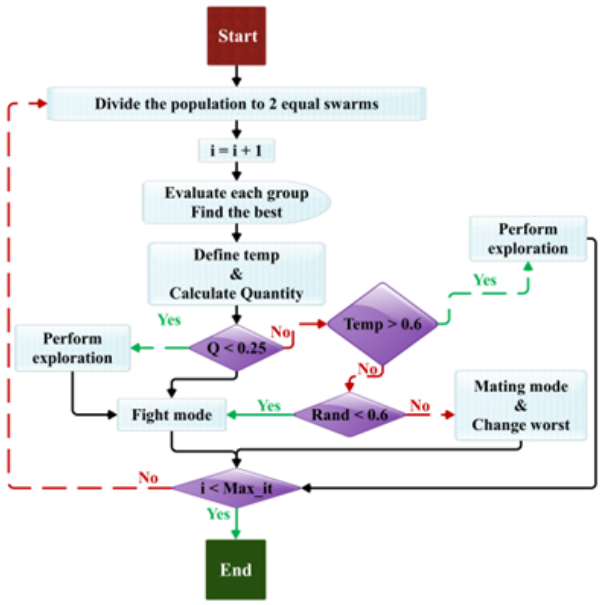

Fig. 3. The SO flowchart

2.4. Adaptive Opposition Slime Mould Algorithm (AOSM)

The SMA, a stochastic optimizer, uses the plasmodial slime mold oscillation mode to choose the best answer to a given function. The AOSM method, on the other hand, adapts the technique behavior of slime mold to the environment by merging opposition-based learning and adaptive decision-making processes. This leads to better solutions for a broader set of challenges. These algorithms are illustrations of bio-inspired optimization techniques, which use biological processes as a model to address difficult optimization problems more effectively. Oscillation mode and positive-negative feedback are used by slime mold to determine the optimal path for food contact. If i is an element of the range $[1, N]$, then $Xi = \left(x_i^1, x_i^2, \cdots, x_i^d\right)$ represents the location of the ith slime mold in d-dimensions. For $\forall i \in [1, N]$, the the ith slime's odor or fitness is represented by $f(Xi)$. Assume that the search space has N slime molds, with (UB) serving as the upper boundary and (LB) as the lower boundary. As a result, the following may be used to express the fitness and location of N slime molds at iteration t in Eqs. (15) and (16):

$$X(t) = \begin{bmatrix} x_1^1 & x_1^2 & \cdots & x_1^d \\ x_2^1 & x_2^2 & \cdots & x_2^d \\ \vdots & \vdots & \vdots & \vdots \\ x_n^1 & x_n^d & \cdots & x_n^d \end{bmatrix} = \begin{bmatrix} x_1 \\ x_2 \\ \vdots \\ x_n \end{bmatrix} \tag{15}$$

$$f(x) = [f(x_1), f(x_2), \ldots, f(x_3)] \tag{16}$$

In SMA, Eq. (17) is used to update the slime mold's location for the next iteration $(t+1)$.

$$X_i(t+1) = \begin{cases} \text{rand.}\ (UB - LB) + LB, r_1 < z \\ X_{lb}(t) + vb \cdot (W \cdot X_A(t) - X_B(t)), r_1 \geq \delta \text{ and } r_2 < p_i \\ vc \cdot x_i(t), r_1 > \delta \text{ and } r_2 \geq p_i \end{cases} \tag{17}$$

The random velocity factors are vb and vc, and the weight factor is W. The person in the local population with the highest fitness value is indicated by the symbol X_{LB}. From the existing population, two slime molds, X_A and X_B, are chosen at random to represent [29]. δ represents the fixed chance of the slime mold initializing at a random search position, which is 0.03. The interval $[0, 1]$ contains the produced random numbers r_1 and r_2. The best individual or its location is used for the next iteration based on pi, the threshold value of the ith slime mold. UB and LB are the upper and lower boundary, and rand is the random number. In this way, it may be calculated by Eq. (18):

$$P_i = \tanh |f(X_i) - f_{\text{Gbest}}|, \forall i \in [1, N] \tag{18}$$

Eq. (19) determines the global best fitness value (f_{Gbest}), which is dependent on the global best position (X_{Gbest}). The fitness value of the ith slime mold, Xi, is represented by $f(Xi)$

$$f_{\text{Gbest}} = f(X_{\text{Gbest}}) \tag{19}$$

To get the weight W for N slime molds in the current iteration t, apply Eq. (20) as follows:

$$\text{W}(\text{sortInd}\, f(i)) = \begin{cases} 1 + \text{rand} \cdot \log\left(\frac{f_{\text{Lbest}} - f(X_i)}{f_{\text{Lbest}} - f_{\text{Lworst}}} + 1\right) & 1 \leq i \leq \frac{N}{2} \\ 1 - \text{rand} \log\left(\frac{f_{\text{Lbest}} - f(X_i)}{f_{\text{Lbest}} - f_{\text{Lworst}}} + 1\right) & \frac{N}{2} < i \leq N \end{cases} \tag{20}$$

The fitness values are sorted in ascending order while solving a minimization problem, as seen below. Next, the weight W is calculated using the provided equation, where f_{Lworst} denotes the local worst fitness value and f_{Lbest} denotes the value of local best fitness. rand is a random number between 0 and 1 . Based on the fitness value f, which is specified in Eq. (21), both of these values are obtained.

$$\left[\text{sort}_f, \text{sortInd}_f\right] = \text{sort}(f) \tag{21}$$

To ascertain the best local fitness value f_{Lbest} and the related local best individual X_{Lbest} . Take the actions listed below:

$$f_{\text{Lbest}} = f(\text{sortf}(1)) \tag{22}$$

$$X_{\text{Lbest}} = x(\text{ sortf }(1)) \tag{23}$$

Use the following procedures to find the local worst fitness value fLW :

$$f_{\text{Lworst}} = f(\text{sort}\, f(N)) \tag{24}$$

A continuous uniform distribution in the intervals $[-b, b]$ and $[-c, c]$ yields the random velocity factors Vb and Vc, respectively. Use the following process to find the values of b and c for the current iteration, t :

$$b = \text{arctanh}\left(-\left(\frac{t}{T}\right)+1\right) \tag{25}$$

and

$$c = 1 - \frac{t}{T} \tag{26}$$

Opposition-based learning (OBL) is used to improve convergence and prevent becoming trapped in local minima. For every slime mold $(i = 1, 2, \cdots, N)$ in the search space, the position Xn_i is compared with its exact opposite position Xo_i in OBL. The location is updated for the next iteration based on an estimate of the difference. Using the following formula, the predicted value of Xo_i for the $i-th$ slime mold in the $j-th$ dimension is determined:

$$Xo_i^j(t) = \min\left(Xn_i(t)\right) + \max\left(Xn_i(t)\right) - Xn_i^j(t) \tag{27}$$

where $i = 1, 2, \ldots, N$ and $j = 1, 2, \ldots, d$.

The ith slime mold position selected for the minimization issue is denoted by Xsi.

$$Xs_i(t) = \begin{cases} Xo_i(t) & \text{if } f\left(Xo_i(t)\right) < f\left(Xn_i(t)\right) \\ Xn_i(t) & \text{if } f\left(Xo_i(t)\right) \geq f\left(Xn_i(t)\right) \end{cases} \tag{28}$$

In cases when the slime mold is following a previously investigated nutrition route, an adaptive choice technique is employed. This approach takes into account the present fitness

value $f(Xni(t))$ in addition to the matching historical fitness value $f(Xi(t))$. The adaptive decision method of AOSM incorporates OBL to allow for more exploration if needed. This approach, which can be expressed as follows, determines the revised location for the subsequent iteration:

$$X_i(t+1) = \begin{cases} Xn_i(t) \text{ if } f\left(Xn_i(t)\right) \leq f\left(X_i(t)\right) \\ Xs_i(t) \text{ if } f\left(Xn_i(t)\right) > f\left(X_i(t)\right) \end{cases} \tag{29}$$

Through the application of an adaptive decision approach, the AOSM technique efficiently improves the performance of SMA by determining when OBL is required along the search trajectory. Furthermore, Fig. 4 displays the AOSM flowchart.

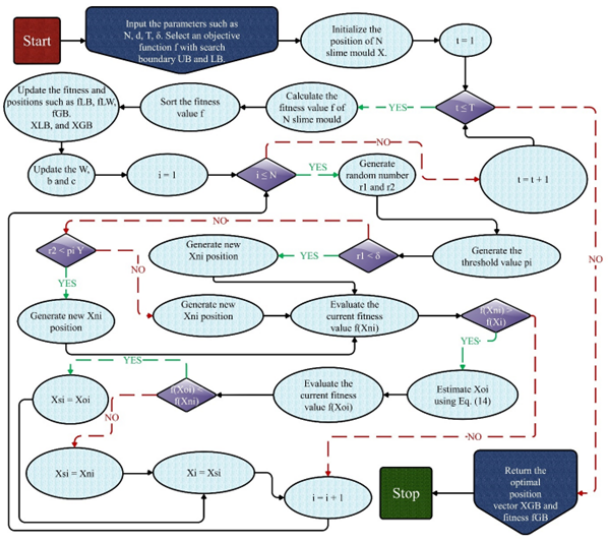

Fig. 4. Flowchart of AOSM

2.5. Performance evaluation methods

This article employs a variety of metrics for assessing the models, containing the previously mentioned Normalized Root Mean Squared Error (NRMSE), Correlation Coefficient $\left(\mathrm{R}^2\right)$, Mean Absolute Error (MAE), Median Absolute Percentage Error (MDAPE), and Root Mean Square Error (RMSE). Excellent performance of the algorithm during the phases of training, validation, and testing is indicated by a high R^2 value. Lower RMSE and MAE values are better since they indicate less model error. These measures are calculated using Eqs. (30) to (34).

- Coefficient of determination

$$R^2 = \left(\frac{\sum_{i=1}^{W}\left(h_i - \bar{h}\right)\left(q_i - \bar{q}\right)}{\sqrt{\left[\sum_{i=1}^{W}\left(h_i - h\right)^2\right]\left[\sum_{i=1}^{W}\left(q_i - \bar{q}\right)^2\right]}}\right)^2 \tag{30}$$

- Root Mean Square Error

$$RMSE = \sqrt{\frac{1}{W}\sum_{i=1}^{W}\left(q_i - h_i\right)^2} \tag{31}$$

- Mean Absolute Error

$$MAE = \frac{1}{W}\sum_{i=1}^{W}\left|q_i - h_i\right| \tag{32}$$

- Normalized Root Mean Squared Error

$$NRMSE = \frac{RMSE}{q_i - \bar{q}} \tag{33}$$

- Median Absolute Percentage Error

$$MDAPE = 100 \times \text{ median}\left(\frac{\left|q_i - \bar{q}\right|}{\left|h_i - \bar{h}\right|}\right) \tag{34}$$

Where q_i and h_i determine the experimental and predicted values, alternatively. The mean values of the predicted and experimental values are shown with $\bar{h}$ and $\bar{q}$, alternatively, W defines the number of samples being considered.

3. Results and discussion

3.1. Hyperparameter and Convergence

Table 2 displays the hyperparameter results for the KNN model, with particular attention to the KNAO and KNSO variants. The values given to the hyperparameters have an impact on the precision and effectiveness of the predictions, and they are crucial in determining how well the model performs. The KNAO and KNSO models for the n _neighbors hyperparameter share a value of 1 . This parameter highlights the importance of local data points in the modeling process by determining the number of neighbors taken into account when making predictions. Turning now to the leaf_size hyperparameter, the KNSO model has a leaf size of 435 , whereas the KNAO model has a value of 877 . This parameter affects how the KD-tree is built, which affects how efficiently queries are executed. Lastly, there are differences between the two models in the p hyperparameter, which stands for the Minkowski distance's power parameter. KNSO chooses a value of 339 , while KNAO uses a value of 1 , stressing the Manhattan distance. The variations in hyperparameter values highlight the careful adjustments made to maximize each model's prediction of heating load performance. This table offers insightful information about the customized hyperparameter configuration for the KNN models that are being examined.

Table 2. The results of hyperparameters for KNN

Hyperparameter	Models	
	KNAO	KNSO
n_neighbors	1	1
leaf_size	877	435
p	1	339

The convergence (RMSE) of the KNAO and KNSO hybrid models is shown in Fig. 5. The RMSE values of the two models as a function of iteration number are displayed in the vertical line plot. The RMSE represents the average difference between the expected and actual values. Lower RMSE values indicate greater accuracy. The graph indicates that the KNAO model has better convergence than the KNSO model. This suggests that a lower RMSE value is reached by the KNAO model more quickly. Put differently, the KNAO model exhibits enhanced efficacy in learning from the training set and yields higher precision predictions. The inclusion of the SO and the AOSMA metaheuristic algorithms in the KNAO model is responsible for its superior convergence. With the help of these algorithms, the search space is more thoroughly explored, enabling the KNAO model to determine the ideal KNN model parameters. The study's findings show that the KNAO model is a viable method for estimating heating load. The KNAO model's superior convergence suggests that it can be used to predict heating loads more accurately, which can lead to increased building energy efficiency.

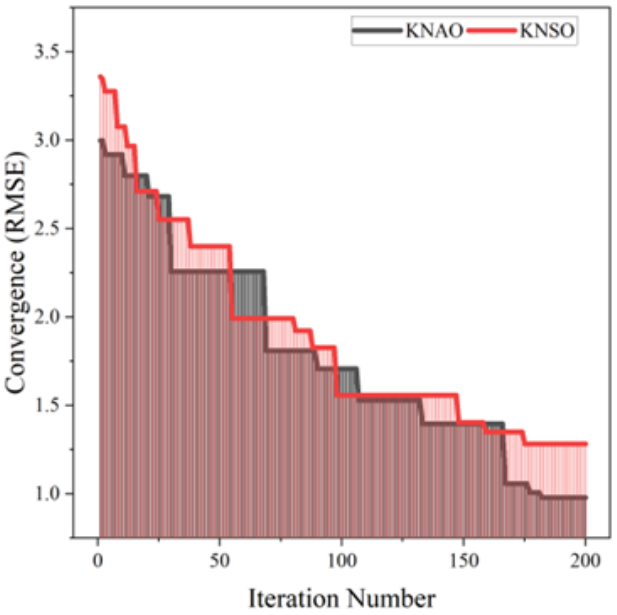

Fig. 5. Vertical line plot for convergence of hybrid models

3.2. Evaluation of developed models

The evaluation of heating load prediction entails a structured four-stage process: training (70%), validation (15%), test (15%), and an overarching assessment (100%). Within this framework, Table 3 and Fig. 6 comprehensively analyze the performance of three distinct K-nearest neighbors (KNN) models: KNN, KNAO, and KNSO, with a focal point on their predictive capabilities regarding heating load. These stages collectively provide insights into the efficacy and suitability of each model for precise heating load predictions, facilitating informed decision-making in various applications.

- RMSE and R^2 : In predictive accuracy, two pivotal metrics, RMSE and R^2, were scrutinized. The KNAO model shone brightly during the training phase, displaying the lowest RMSE and the highest R^2 values (0.800 and 0.994 , respectively). These statistics under-

Table 3. The result of developed models

Model	Section	Index values				
		RMSE	R^2	MAE	NRMSE	MDAPE
KNN	Train	1.599	0.976	1.001	0.003	2.430
	Validation	2.195	0.951	1.401	0.019	3.706
	Test	1.747	0.970	1.210	0.015	3.710
	All	1.723	0.971	1.092	0.002	2.704
KNAO	Train	0.800	0.994	0.705	0.001	3.132
	Validation	1.305	0.983	1.038	0.011	4.437
	Test	1.306	0.983	1.114	0.011	4.640
	All	0.979	0.991	0.816	0.001	3.556
KNSO	Train	1.157	0.987	1.001	0.002	4.600
	Validation	1.435	0.981	0.916	0.012	2.635
	Test	1.636	0.977	1.085	0.014	2.845
	All	1.283	0.984	1.001	0.002	3.889

score its exceptional fit and predictive prowess during this phase. In contrast, the KNN model demonstrated consistent performance across all three phases, a testament to its reliability in RMSE and R^2 values.

- MAE and NRMSE: Expanding the scope of assessment, MAE and NRMSE were analyzed. Surprisingly, the KNN and KNSO models presented higher error rates across all phases. However, the KNAO model emerged as the standout performer during the training phase, boasting a significantly lower MAE of 0.705 and an exceptionally low NRMSE of 0.001.

- MDAPE: The MDAPE metric was pivotal in gauging predictive accuracy. Notably, the KNN model consistently exhibited the highest MDAPE across all phases, affirming its superior predictive accuracy. It is worth noting that the KNAO model showcased a lower MDAPE value exclusively during the training phase, indicating its competitive edge in this specific context.

In essence, the selection among the KNN, KNAO, and KNSO models depends on the unique demands of each application. The KNAO model stands out for its exceptional predictive accuracy, particularly during training. Conversely, the KNN model offers consistent performance and precision in estimating absolute errors across all phases. Meanwhile, the

KNSO model strikes a harmonious balance between accuracy and predictive power. This thorough assessment empowers decision-makers to choose the optimal model for precise heating load predictions, tailored to their priorities of precision, reliability, or a blend of both.

The study assesses the efficacy of hybrid models throughout the training, validation, and testing phases, as illustrated in the scatter plot depicted in Fig. 7. Notably, the KNAO model demonstrates robust accuracy consistently, displaying minimal deviation between predicted and observed values. Conversely, both the KNN and KNSO models exhibit comparable performance, albeit with slightly diminished precision and increased inaccuracy, as evidenced by their data points positioned further from the centerline. This wider dispersion implies a marginally lower precision and heightened inaccuracy compared to the KNAO model.

A line plot of the error percentages related to the developed models is shown in Fig. 8. KNAO has the lowest error of 19.81, as the graph demonstrates, with the majority of values clustered around the 10% range. The error percentages for KNN and KNSO, on the other hand, exhibit a broader distribution, with a significant concentration of values greater than 33.33% and 37.14%. The fact that the KNN and KNSO distributions are right-skewed is significant because they indicate that some dataset points have noticeably higher error rates. This result demonstrates the high accuracy of KNAO and demonstrates how the developed models' error percentage distributions are displayed in the graph.

Fig. 9 displays a violin plot with box plots representing the error percentages for the models under examination. The graph effectively accentuates the unique characteristics of each model. KNAO exhibits a sharply peaked normal distribution with minimal spread, resulting in an average error range between -20% and 20%. In contrast, KNN displays greater dispersion and a flatter normal distribution across all three phases, but it performs optimally when its error range falls within -25% to 35%. KNSO stands out due to its pronounced and varied errors, including an outlier data point contributing to an error range of -22% to 30% of the dataset. Conversely, KNN demonstrates a more

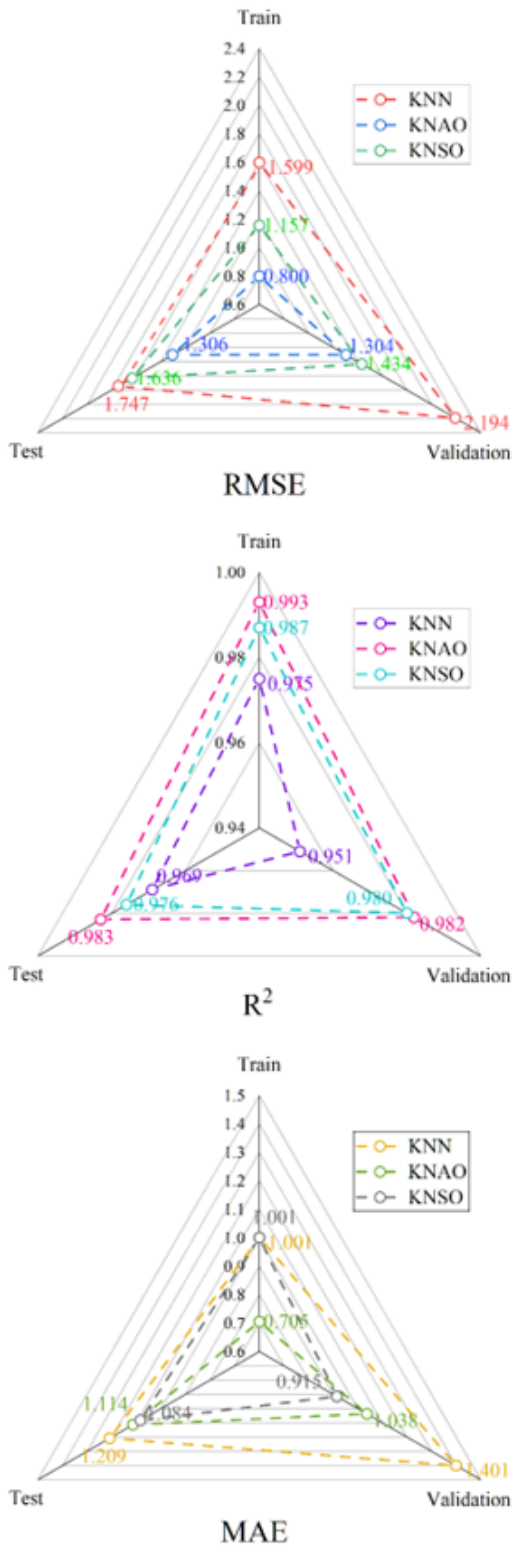

Fig. 6. The radar plot for presented metrics

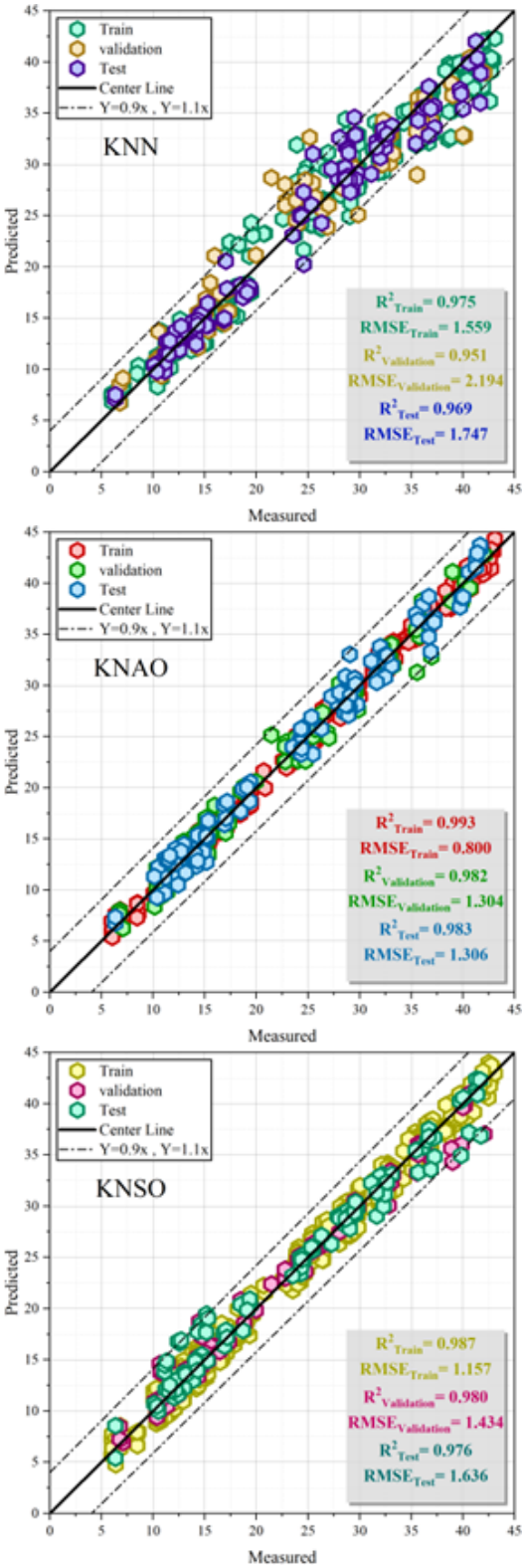

Fig. 7. Plotting developed hybrid models' dispersion

evenly distributed error pattern than the other two models, with a reduced occurrence of errors clustering around zero. Notably, the results of this study unequivocally establish KNAO as the most effective model, underscoring its supe-

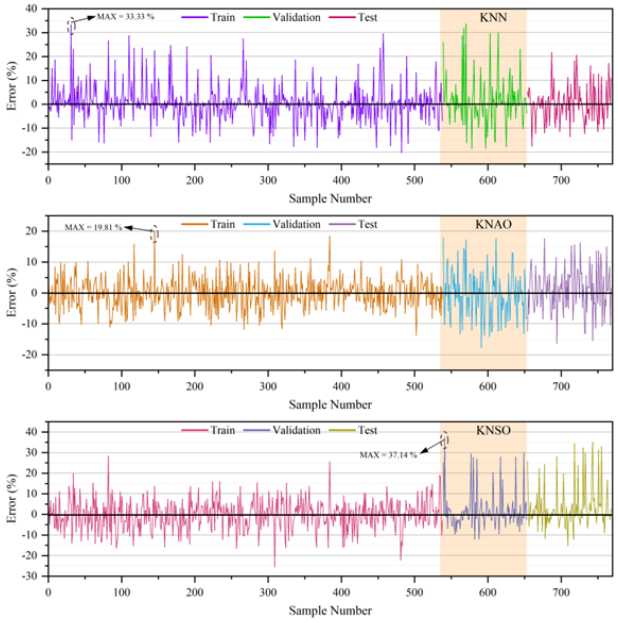

Fig. 8. The line plot is the basis for the models' error percentage

rior ability to minimize dispersion and reduce error rates consistently across all scenarios.

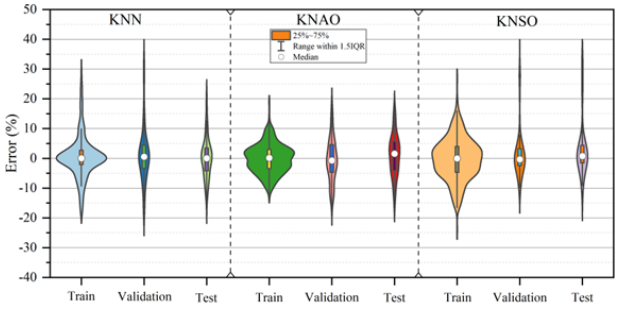

Fig. 9. The violin with box plot errors of proposed models

In Fig. 10, a Taylor diagram is used to compare the performance of several models. The study assesses three models, KNN, KNAO, and KNSO for predicting heating load. The diagram's horizontal axis shows the standard deviation of expected values from each model, while the radial axis shows the correlation coefficient between observed and anticipated values. Distance from the origin indicates a higher standard deviation in model predictions. Closer to the circle, with a correlation value of 1, indicates better model performance. The graphic shows that the KNAO model has the greatest correlation coefficient (0.99) and a standard deviation of 0.5. The KNAO model shows a great correlation with observed values and low variance in forecasts.

In contrast, the KNSO model has a correlation value of around 0.95 and a standard deviation approaching 1. The KNN model has the lowest correlation coefficient (0.9) and the biggest standard deviation (1.5). Overall, the graphic shows that the KNAO model predicts heating load better than the other three models.

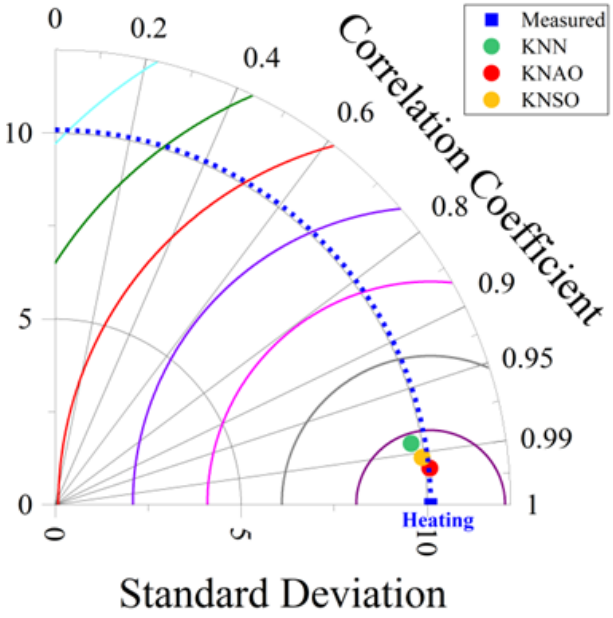

Fig. 10. The Taylor diagram of related models

4. Conclusion

This research delves deeply into machine learning (ML) approaches, specifically focusing on K-Nearest Neighbors (KNN) based models, with the primary goal of enhancing energy efficiency and optimizing heating systems in residential buildings. The overarching aim was to achieve highly accurate heat load forecasts in home environments. The study also delved into optimization methods, particularly investigating the Adaptive Opposition Slime Mould Algorithm (AOSMA) and the Snake Optimizer (SO) to further refine and improve these KNN models. Through this investigation, several significant findings have come to light: Firstly, the KNN models have demonstrated their invaluable utility in estimating heat load in residential buildings. Trained on relevant data, these models showcased a remarkable ability to make precise predictions, providing crucial insights into the energy requirements of such structures.

Their simplicity and interpretability make them particularly appealing for practical applications. The assessment process, covering training, validation, testing, and comprehensive evaluation stages, rigorously analyzed each

model's performance using various metrics such as RMSE, R^2, MAE, NRMSE, and MDAPE. These metrics offered nuanced insights into the predictive proficiency and accuracy of the models across different evaluation phases. Distinct performance characteristics emerged for each model. The KNAO model stood out as a top performer during the training phase, demonstrating the lowest RMSE value 0.8003 of and the highest R^2 value of 0.993 , indicating exceptional predictive capabilities. Conversely, the KNN model showed consistent performance across all phases, showcasing reliability in estimating heating load but with scope for improvement in predictive accuracy. The KNSO model struck a balance between accuracy and predictive power, delivering competitive performance across various metrics. The integration of optimization algorithms, especially with the KNN model using AOSMA, yielded significant improvements in accuracy and reduced prediction errors. This integration holds promise for enhancing predictive performance, leading to more sustainable and efficient home heating systems.

In conclusion, combining ML techniques like KNN models with optimization algorithms such as AOSMA and SO has the potential to revolutionize energy efficiency in residential buildings. This fusion enables a sustainable and efficient future for heating systems, paving the way for smarter and greener living environments. Tailoring model selection based on specific application needs further enhances the overall effectiveness and applicability of these approaches in real-world scenarios.

5. Limitation

This study uses ML approaches, including KNN models, to improve energy efficiency and optimize heating systems in residential settings. The main goal is to anticipate heat load in these situations accurately. Explore integrating optimization methods like SO and AOSMA to improve KNN model effectiveness. The study demonstrates the reliability of KNN models in calculating heat load in residential structures. These models, trained on appropriate datasets, provide beneficial insights into energy needs due to their simplicity and interpretability. The use of optimization techniques like SO and AOSMA enhances the predicted accuracy of these models. When used with KNN, AOSMA excels, achieving high precision and minimum prediction mistakes. The ability to cluster data points and uncover substantial correlations highlights the potential for optimization algorithms to improve prediction capabilities. The study suggests that integrating ML, particularly KNN models, with optimization algorithms like AOSMA and SO could change household energy efficiency tactics. The success of the AOSMA concept suggests a sustainable and efficient future for domestic heating systems. Effective heat load prediction and system optimization can significantly reduce energy consumption and emissions, promoting environmental sustainability and perhaps cutting homeowner expenses. This research enables the use of modern technology in domestic energy management, promoting a greener and more efficient built environment.

6. Funding

This work was supported by Research and development of data management integration for intelligent control equipment of Industrial wastewater treatment based on a deep learning algorithm (KYP022204).

nomenclature

Acronyms

AI	Artificial intelligent
AOSMA	Adaptive Opposition Slime Mould Algorithm
GA	Glazing Area
GAD	Glazing Area Distribution
HL	Heating load
HVAC	Heating, ventilation, and air conditioning
KNN	K-Nearest Neighbor
MAE	Mean Absolute Error
MAPE	Median Absolute Percentage Error
ML	Machine learning
NRMSE	Normalized Root Mean Square Error
OR	Orientation
OVH	Overall Height
R^2	Coefficient Correlation
RA	Roof Area
RCE	Relative Compactness
RMSE	Root Mean Square Error
SA	Surface Area
SO	Snake Optimizer
WA	Wall Area

References

[1] M. R. Biswas, M. D. Robinson, and N. Fumo, (2016) *"Prediction of residential building energy consumption: A neural network approach"* **Energy *117***: 84–92.

[2] B. Sadaghat, A. Javadzade Khiavi, B. Naeim, E. Khajavi, H. Sadaghat, and A. R. Taghavi Khanghah, (2023) *"The utilization of a naive bayes model for predicting the energy consumption of buildings"* **Journal of Artificial Intelligence and System Modelling *1***(01): 73–91.

[3] M. Protić, S. Shamshirband, M. H. Anisi, D. Petković, D. Mitić, M. Raos, M. Arif, and K. A. Alam, (2015) *"Appraisal of soft computing methods for short term consumers' heat load prediction in district heating systems"* **Energy** *82*: 697–704.

[4] Y. Ding, Q. Zhang, T. Yuan, and F. Yang, (2018) *"Effect of input variables on cooling load prediction accuracy of*

an office building" **Applied Thermal Engineering *128***: 225–234.

[5] Q. Zhang, Z. Tian, Z. Ma, G. Li, Y. Lu, and J. Niu, (2020) *"Development of the heating load prediction model for the residential building of district heating based on model calibration"* **Energy *205***: 117949.

[6] G. Xue, C. Qi, H. Li, X. Kong, and J. Song, (2020) *"Heating load prediction based on attention long short term memory: A case study of Xingtai"* **Energy *203***: 117846.

[7] A. T. C. on Application of Artificial Neural Networks in Hydrology, (2000) *"Artificial neural networks in hydrology. II: Hydrologic applications"* **Journal of Hydrologic Engineering *5***: 124–137.

[8] Z.-H. Zhou. *Machine learning*. Springer nature, 2021.

[9] S. Afzal, B. M. Ziapour, A. Shokri, H. Shakibi, and B. Sobhani, (2023) *"Building energy consumption prediction using multilayer perceptron neural network-assisted models; comparison of different optimization algorithms"* **Energy *282***: 128446.

[10] H. Wang, Z. Lei, X. Zhang, B. Zhou, and J. Peng, (2016) *"Machine learning basics"* **Deep learning**: 98–164.

[11] S. M. Weiss and C. A. Kulikowski. *Computer systems that learn: classification and prediction methods from statistics, neural nets, machine learning, and expert systems*. Morgan Kaufmann Publishers Inc., 1991.

[12] Q. Zhang, Z. Tian, Z. Ma, G. Li, Y. Lu, and J. Niu, (2020) *"Development of the heating load prediction model for the residential building of district heating based on model calibration"* **Energy *205***: 117949.

[13] E. Guelpa, L. Marincioni, M. Capone, S. Deputato, and V. Verda, (2019) *"Thermal load prediction in district heating systems"* **Energy *176***: 693–703.

[14] S. Shamshirband, D. Petković, R. Enayatifar, A. H. Abdullah, D. Marković, M. Lee, and R. Ahmad, (2015) *"Heat load prediction in district heating systems with adaptive neuro-fuzzy method"* **Renewable and Sustainable Energy Reviews *48***: 760–767.

[15] A. N. Sharif, S. K. Saleh, S. Afzal, N. S. Razavi, M. F. Nasab, and S. Kadaei, (2022) *"Evaluating and Identifying Climatic Design Features in Traditional Iranian Architecture for Energy Saving"*:

[16] B. Sadaghat, S. Afzal, and A. J. Khiavi, (2024) *"Residential building energy consumption estimation: A novel ensemble and hybrid machine learning approach"* **Expert Systems with Applications *251***: 123934.

[17] I. Jaffal, C. Inard, and C. Ghiaus, (2009) *"Fast method to predict building heating demand based on the design of experiments"* **Energy and Buildings *41***: 669–677.

[18] P. J. G. Nieto, E. García–Gonzalo, F. S. Lasheras, J. P. Paredes–Sánchez, and P. R. Fernández, (2019) *"Forecast of the higher heating value in biomass torrefaction by means of machine learning techniques"* **Journal of Computational and Applied Mathematics *357***: 284–301.

[19] G. Xue, C. Qi, H. Li, X. Kong, and J. Song, (2020) *"Heating load prediction based on attention long short term memory: A case study of Xingtai"* **Energy *203***: 117846.

[20] Y. Ding, Q. Zhang, T. Yuan, and K. Yang, (2018) *"Model input selection for building heating load prediction: A case study for an office building in Tianjin"* **Energy and Buildings *159***: 254–270.

[21] T.-Y. Kim and S.-B. Cho, (2019) *"Predicting residential energy consumption using CNN-LSTM neural networks"* **Energy *182***: 72–81.

[22] A. Moradzadeh, A. Mansour-Saatloo, B. Mohammadi-Ivatloo, and A. Anvari-Moghaddam, (2020) *"Performance evaluation of two machine learning techniques in heating and cooling loads forecasting of residential buildings"* **Applied Sciences *10***: 3829.

[23] S. S. Roy, P. Samui, I. Nagtode, H. Jain, V. Shivaramakrishnan, and B. Mohammadi-Ivatloo, (2020) *"Forecasting heating and cooling loads of buildings: A comparative performance analysis"* **Journal of Ambient Intelligence and Humanized Computing *11***: 1253–1264.

[24] S. Afzal, B. M. Ziapour, A. Shokri, H. Shakibi, and B. Sobhani, (2023) *"Building energy consumption prediction using multilayer perceptron neural network-assisted models; comparison of different optimization algorithms"* **Energy *282***: 128446.

[25] L. Xiong and Y. Yao, (2021) *"Study on an adaptive thermal comfort model with K-nearest-neighbors (KNN) algorithm"* **Building and Environment *202***: 108026.

[26] H. A. A. Alfeilat, A. B. A. Hassanat, O. Lasassmeh, A. S. Tarawneh, M. B. Alhasanat, H. S. E. Salman, and V. B. S. Prasath, (2019) *"Effects of distance measure choice on k-nearest neighbor classifier performance: a review"* **Big data *7***: 221–248.

[27] S. Uddin, I. Haque, H. Lu, M. A. Moni, and E. Gide, (2022) *"Comparative performance analysis of K-nearest neighbour (KNN) algorithm and its different variants for disease prediction"* **Scientific Reports *12***: 6256.

[28] F. A. Hashim and A. G. Hussien, (2022) *"Snake Optimizer: A novel meta-heuristic optimization algorithm"* **Knowledge-Based Systems *242***: 108320.

[29] O. Altay, (2022) *"Chaotic slime mould optimization algorithm for global optimization"* **Artificial Intelligence Review *55***: 3979–4040.